Cole-Carpenter Syndrome Is Caused by a Heterozygous Missense Mutation in *P4HB*

Frank Rauch,[1,*] Somayyeh Fahiminiya,[2] Jacek Majewski,[2] Jian Carrot-Zhang,[2] Sergei Boudko,[3] Francis Glorieux,[1] John S. Mort,[1] Hans-Peter Bächinger,[3] and Pierre Moffatt[1]

Cole-Carpenter syndrome is a severe bone fragility disorder that is characterized by frequent fractures, craniosynostosis, ocular proptosis, hydrocephalus, and distinctive facial features. To identify the cause of Cole-Carpenter syndrome in the two individuals whose clinical results were presented in the original description of this disorder, we performed whole-exome sequencing of genomic DNA samples from both individuals. The two unrelated individuals had the same heterozygous missense mutation in exon 9 of *P4HB* (NM_000918.3: c.1178A>G [p.Tyr393Cys]), the gene that encodes protein disulfide isomerase (PDI). In one individual, the *P4HB* mutation had arisen de novo, whereas in the other the mutation was transmitted from the clinically unaffected father who was a mosaic carrier of the variant. The mutation was located in the C-terminal disulfide isomerase domain of PDI, sterically close to the enzymatic center, and affected disulfide isomerase activity in vitro. Skin fibroblasts showed signs of increased endoplasmic reticulum stress, but despite the reported importance of PDI for collagen type I production, the rate of collagen type I secretion appeared normal. In conclusion, Cole-Carpenter syndrome is caused by a specific de novo mutation in *P4HB* that impairs the disulfide isomerase activity of PDI.

Cole-Carpenter syndrome (CCS; MIM 112240) was first identified by Cole and Carpenter in 1987 who described two unrelated boys with a strikingly similar phenotype that was characterized by "bone fragility, craniosynostosis, ocular proptosis, hydrocephalus, and distinctive facial features."[1] They called this disorder "a newly recognized type of osteogenesis imperfecta" (OI), but the term "Cole-Carpenter syndrome" has usually been used to refer to this condition.[2] After the initial description of the syndrome, only one other similar case has been reported.[3] Despite its apparent extreme rarity, CCS is commonly classified as a separate OI-like disorder.[4–6]

OI is usually transmitted in an autosomal dominant fashion and is mostly caused by mutations in *COL1A1* (MIM 120150) or *COL1A2* (MIM 120160), the genes encoding collagen type I alpha chains.[7] Other dominantly and recessively inherited forms of OI are rare and can be caused by mutations in a variety of genes (*BMP1* [MIM 112264], *CRTAP* [MIM 605497], *FKBP10* [MIM 607063], *IFITM5* [MIM 614757], *LEPRE1* [MIM 610339], *PPIB* [MIM 123841], *SERPINF1* [MIM 172860], *SERPINH1* [MIM 600943], *SP7* [MIM 606633], *TMEM38B* [MIM 611236], *WNT1* [MIM 164820]), which are either involved in the post-translational modification of collagen type I or in the regulation of osteoblast function.[8] Collagen type I protein analyses in skin fibroblasts were reportedly normal in the two individuals with CCS where this test was performed.[1,3] No further investigations into the molecular cause of CCS have been reported. The gene defect underlying CCS is thus unclear.

The clinical course of the two individuals described by Cole and Carpenter was initially reported up to the ages of 4 years and 19 months, respectively.[1] Both were later evaluated in our institution (Table S1). Individual 1 was born to unrelated healthy parents at term and sustained multiple fractures in the first few months of life. Progressive proptosis and frontal bossing developed in the following months. Craniosynostosis of the coronal and frontal sutures was diagnosed and frontal craniectomy was performed. Communicating hydrocephalus was noted at 12 months of age requiring a ventriculo-peritoneal shunt. Teeth were small and had hypoplastic enamel. When individual 1 was 3 years old, craniofacial surgery was performed in an attempt to reduce facial deformities. At 4 years of age, he had normal cognitive development and, following intramedullary rodding surgery of the left femur, was able to stand. We first evaluated individual 1 when he was 18 years old. He was using a wheelchair for all mobility and had severe scoliosis and marked deformity of the upper and lower extremities. Height was 120 cm (Z score: −8.4) and lumbar spine areal bone mineral density was low (Z score: −3.9). Serum levels of calcium, inorganic phosphorus, creatinine, alkaline phosphatase, and parathyroid hormone were normal. He received four cycles of intravenous pamidronate infusions over a 12-month period, with no obvious change in clinical status, even though lumbar spine areal bone mineral density Z score increased to −2.4.

Individual 2 was the only son of healthy and nonconsanguineous parents. He was brought to medical attention at 2 months of age, when the presence of several fractures, micrognathia, frontal bossing, and ocular proptosis were noted. The anterior fontanel was very large and contiguous with the posterior fontanel. He developed communicating hydrocephalus in the first 18 months of life. He first presented at our institution at 18 years of

[1]Shriners Hospital for Children, Montréal, QC H3G 1A6, Canada; [2]Department of Human Genetics, McGill University and Génome Québec Innovation Centre, Montréal, QC H3A 1B1, Canada; [3]Shriners Hospital for Children, Portland, OR 97239, USA
*Correspondence: frauch@shriners.mcgill.ca
http://dx.doi.org/10.1016/j.ajhg.2014.12.027.

Figure 1. Radiographic Findings in Individual 2 at 18 Years of Age
(A) Lateral skull radiograph showing severe midface hypoplasia.
(B) The right upper extremity is severely deformed.
(C) In the lower extremities, both femurs and tibias have undergone intramedullary rodding surgery. Epiphyses of both distal femurs are wide and seem filled with nodular structures ("popcorn epiphyses"). The right femur shows a large cystic area (asterisk) and no bone is visible in the midshaft area (arrow).
(D) Wide epiphyses of the metacarpal and digital bones, thin cortices and a cystic appearance. Some of the end phalanges seem to be partially resorbed (arrows).

age, with severe scoliosis and marked deformity of the upper and lower extremities with "popcorn epiphyses" in the distal femur and proximal tibia (Figure 1). He used a wheelchair for all mobility. Height was 97 cm (Z score: −11.7) and lumbar spine areal bone mineral density Z score was −5.1. Serum levels of calcium, inorganic phosphorus, creatinine, alkaline phosphatase, and parathyroid hormone were normal. Intravenous pamidronate treatment, given for 3 years, was associated with an increase in lumbar spine areal bone mineral density Z score to −4.2, and otherwise unchanged clinical status.

Because of the strikingly similar phenotypes of individuals 1 and 2, we hypothesized that the same gene was mutated in both. Aiming at the identification of the disease-causing genetic variant, we performed whole-exome sequencing on genomic DNA of both men after obtaining approval from the Institutional Review Board of McGill University and informed consent from the two individuals. We used Agilent SureSelect Human All Exon Kit version 4 for target enrichment, and 100 bp paired-end runs on an Illumina HiSeq 2000 device at Genome Quebec and McGill University Innovation Center, Montreal, Canada, as previously detailed.[9] The bioinformatics analysis of exome sequencing data was carried out as described previously.[10,11] Briefly, we used BWA (v. 0.5.9) for mapping of 100 base pair paired-end reads against the human reference genome (hg19), Samtools mpileup (version 0.1.17) for variant calling, and ANNOVAR[12] for variants annotation. A mean coverage of 176X (individual 1) and 139X (individual 2) was obtained for all consensus coding sequence exons, and 93% of bases were covered by ≥20 reads as determined by the Genome Analysis Toolkit. In order to focus on likely disease-causing variants, we filtered out the variants with an allele frequency >5% in either the 1000 Genomes database or the NHLBI/NHGRI Exome Project (v.0.0.14, June 20, 2012). We also filtered out variants that had previously been seen in >10 individuals in our exome database (over 1,000 exomes). Finally, we only considered the most protein damaging variants (frameshift indel, nonsense, missense, and canonical splice site) for further analysis. This shortlisted 329 and 336 variants in individuals 1 and 2, respectively.

We first investigated the occurrence of rare variants in the aforementioned genes that are known to be associated with autosomal dominant and recessive OI. Only individual 1 carried a nonsynonymous heterozygous variant in *SERPINH1* (NM_001235.3:c.689A>G [p.Tyr230Cys]). Although, mutations in this gene were previously linked to an autosomal recessive form of OI, heterozygous carriers were reported to be phenotypically healthy.[13] Thus, we concluded that this variant could not be responsible for the syndrome.

Aiming at the identification of a protein-coding gene that was mutated in both individuals, we combined exome data from both individuals and identified 5 candidate genes (Table S2). This revealed that the same nonsynonymous heterozygous c.1178A>G (p.Tyr393Cys) variant in exon 9 of *P4HB* (MIM 176790; NM_000918.3) was mutated in both individuals (Figure S1). This variant was not present in the databases of dbSNP, 1000 Genomes, the NHLBI/NHGRI Exome Project, or the Exome Aggregation Consortium and was not previously seen in our in-house exome database. Moreover, it was predicted to be damaging by three different bioinformatics algorithms (SIFT,[14] PolyPhen-2,[15] MutationTaster[16]).

Sanger sequencing confirmed that individual 1 (II-1 in Family 1, Figure 2A) and individual 2 (II-1 in Family 2) were both heterozygous for the c.1178A>G change in *P4HB*. Sanger sequencing also revealed that neither of the parents of individual 2 had this variant, suggesting

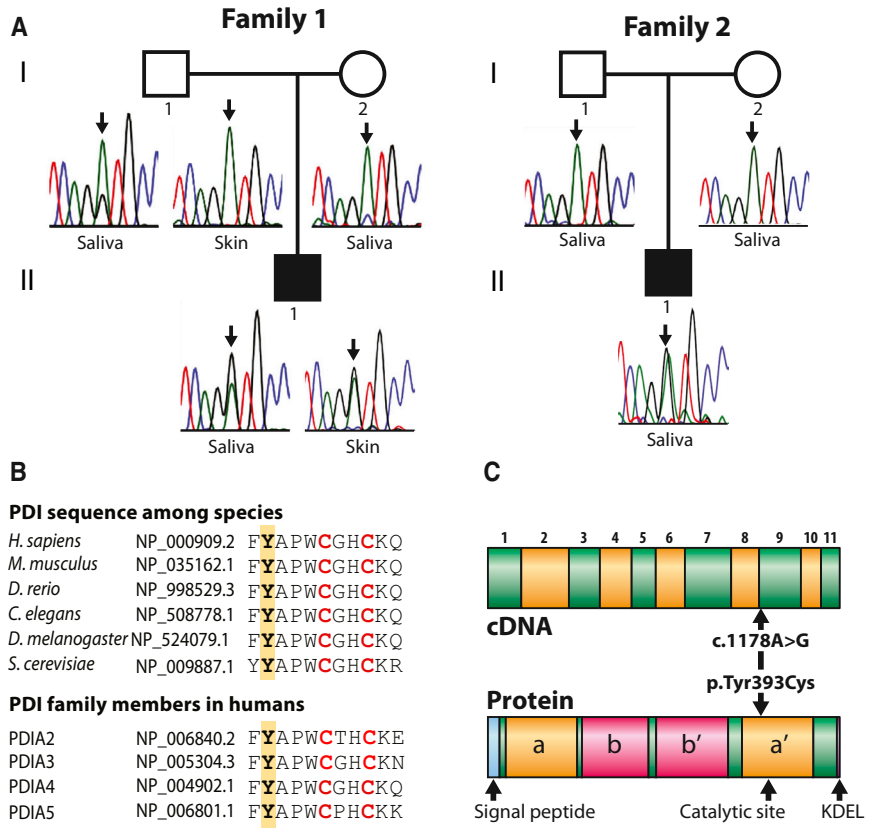

Figure 2. Confirmation of the Heterozygous *P4HB* Mutation in Individuals 1 and 2, and Prediction of Its Impact on PDI

(A) Pedigrees of the families of individual 1 (II-1 in family 1) and individual 2 (II-1 in family 2) and Sanger sequencing chromatogram at the site of c.1178A in *P4HB* (indicated by arrows). Individuals 1 and 2 are heterozygous for the c.1178A>C variant. The chromatograms of the father of individual 1 indicate the presence of the c.1178A>C variant with a lower relative peak size in DNA extracted from saliva, but not in DNA extracted from skin fibroblasts.

(B) Amino acid conservation of the Tyr393 residue in PDI (NP_000909.2). Tyr393 and the following 8 residues are perfectly conserved among species. Tyrosine at the corresponding position is also conserved among the various PDI family members.

(C) Schematic representation of PDI and of the coding exons of *P4HB* cDNA (NM_000918.3). The locations of the exons are aligned relative to the regions of PDI that each exon encodes. The position of the mutation reported in the present study is indicated. The domains of PDI are represented by a, b, b′, a′. An endoplasmic reticulum retention motif (KDEL) is present at the C terminus.

(D) Model of the critical region in PDI. Cys397 and Cys400 are the active site residues, which normally form a reversible disulfide bond. When Tyr393 is mutated to Cys393, the new Cys393 is sterically close to Cys400 and thus might interfere with the active site of PDI.

that the mutation had arisen de novo in individual 2. In the father of individual 1 (I-1 in Family 1), Sanger sequencing of genomic DNA extracted from saliva indicated a c.1178A>G nucleotide change (Figure 2A). However, the relative height of the peak corresponding to the variant nucleotide was lower than in his son, suggesting that the father was mosaic for this mutation. Quantification with PeakPicker software[17] indicated that this individual carried the variant in 23% of cells present in saliva. However, the variant was not found in genomic DNA extracted from his skin fibroblasts (Figure 2A). Because he denied any medical problems, and in particular had not suffered any fractures, no further evaluations were performed.

The mutation rate for single nucleotide variants is in the order of 1–2 × 10^{-8} and therefore between 0 and 2 de novo mutations are typically found in an exome.[18,19] Consequently, the probability of finding the identical de novo mutation in both family 1 and family 2 by coincidence is less than 10^{-7}. We therefore concluded that the c.1178A>G change in *P4HB* was the disease-causing variant in individuals 1 and 2.

The c.1178A>G variant affects the first nucleotide of *P4HB* exon 9. In order to rule out an effect of the mutation on splicing, we obtained cDNA from skin fibroblasts of individuals 1 and 2 and performed PCR using primers in exons 8 and 10 of *P4HB*. Gel electrophoresis of the resulting PCR products revealed a single band of the expected length (Figure S2), suggesting that splicing was not affected. We therefore concluded that the c.1178A>G variant led to a p.Tyr393Cys amino acid substitution in protein disulfide isomerase (PDI; NP_000909.2), the protein encoded by *P4HB*. The affected amino acid residue is perfectly conserved in the PDI of eukaryotic organisms and also in other members of the PDI protein family, thus indicating the functional importance of this residue throughout evolution (Figure 2B).

PDI is the ubiquitously expressed prototypical member of the disulfide isomerase family of proteins, which assist

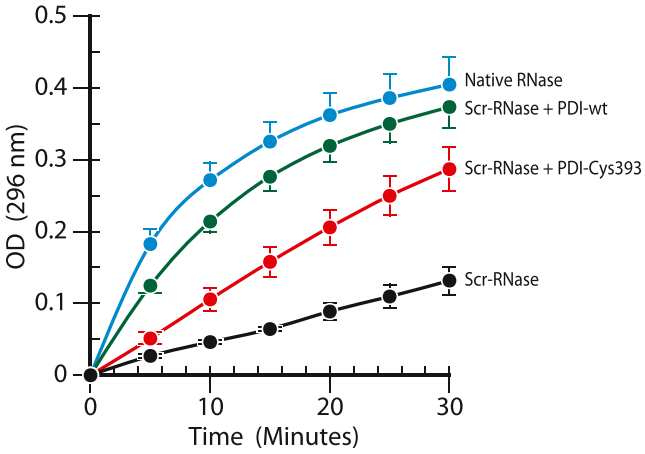

Figure 3. Effect of the p.Tyr393Cys Variant on the Disulfide Isomerase Activity of PDI
Scrambled RNase A (Scr-RNase) was incubated for 5 min with 1.0 μM of either wild-type PDI (PDI-wt) or PDI carrying the p.Tyr393Cys variant (PDI-Cys393). RNase activity (final RNase A concentration: 4 μM) was determined by adding cytidine 2′,3′-cyclic monophosphate (cCMP, Sigma-Aldrich) (final concentration: 2 mM). The hydrolysis of cCMP by active RNase A was monitored by measuring the absorbance at 296 nm. Changes in absorbance (means and SE of four independent experiments) are shown every 5 min.

with the correct formation of disulfide bridges in nascent polypeptide chains and therefore are key enzymes for protein folding.[20,21] PDI also has important functions during the posttranslational modification of procollagen type I, acting as a chaperone to prevent aggregation of procollagen alpha chains, and as a support for the procollagen prolyl 4-hydroxylase alpha subunit, the protein that hydroxylates many proline residues on the procollagen type I alpha chains.[22,23] PDI is therefore also referred to as prolyl 4-hydroxylase beta subunit.

The fundamental importance of PDI for eukaryotic organisms is highlighted by the fact that PDI is essential for cell viability in yeast.[24] It therefore appears likely that global PDI deficiency is embryologically lethal in mammalians. In accordance with this hypothesis, mice with homozygous global PDI deficiency have not been reported.[25] No Mendelian disorders in humans have been linked to mutations in *P4HB*.

PDI comprises two domains (called a and a′) with disulfide isomerase activity (Figure 2C). The p.Tyr393Cys variant is located near the C-terminal reactive center, of which Cys397 and Cys400 are two key residues.[21,26] Protein modeling showed that the cysteine introduced by the p.Tyr393Cys variant is in close sterical proximity to Cys400 (Figure 2D), which led us to hypothesize that the variant interferes with the disulfide isomerase function of the C-terminal reactive center.

To test this hypothesis, we used the scrambled RNase A assay, a widely used method to determine the activity of enzymes with disulfide isomerase activity.[27] Scrambled RNase A contains random disulfide bonds that can be rearranged by disulfide isomerases to the pattern of native RNase, thus reestablishing its molecular conformation and enzymatic activity. RNase activity can then be determined spectrophotometrically. We produced recombinant human full-length wild-type PDI as well as PDI with the p.Tyr393Cys substitution by expression in *E. coli* and compared the ability of the two forms of PDI to reactivate scrambled RNase A. We observed that RNase activity was clearly lower after incubation with PDI carrying the p.Tyr393Cys variant (Figure 3). This confirmed that the p.Tyr393Cys variant impaired the ability of PDI to act as a disulfide isomerase.

We next assessed the effects of the p.Tyr393Cys variant in skin fibroblasts. Expression of PDI protein appeared quantitatively normal in cells carrying the mutation (Figure 4A). However, when the immunoblot was repeated under non-reducing conditions, thus preserving disulfide bridges, additional bands appeared at higher molecular weight (≥100 kD) in fibroblasts with the mutation. These species were also detected in control cells, but to a much lesser extent. This suggests that PDI-Cys393 forms more stable disulfide bridges with substrate proteins than wild-type PDI.

Because PDI is thought to be important for collagen type I processing, we evaluated collagen type I production in fibroblasts. Delays in collagen type I triple helical formation typically lead to overmodification of collagen alpha chains.[28] However, no obvious abnormality in migration pattern of collagen type I alpha chains was found (Figure S3A), confirming findings that were previously reported by others.[1,3] Pulse-chase experiments indicated a normal rate of secretion of procollagen type I (Figure S3B). Electron microscopy of fibroblast cultures did not show obvious abnormalities in the appearance of either cells or extracellular matrix (data not shown). However, immunofluorescence studies showed a marked increase in the vesicular pattern of both PDI and procollagen type I distribution in CCS fibroblasts, contrasting with the normal reticular and Golgi-like staining observed in control cells (Figure 4B). Immunoblotting showed increased expression of heat shock protein 47, another collagen chaperone molecule, suggesting the presence of endoplasmic reticulum stress (Figure 4C).

This study shows that CCS is caused by a heterozygous de novo mutation in *P4HB* that is identical in the two disease-defining individuals. The resulting p.Tyr393Cys variant leads to a reduction of disulfide isomerase activity in vitro. However, it appears unlikely that the CCS phenotype is simply due to PDI haploinsufficiency in vivo. Inactivating variants in genes coding for enzymes usually do not cause a phenotype when heterozygous. Mice with heterozygous ablation of *P4hb* were generated in at least one study and were viable and fertile.[25] Importantly, heterozygous deletions encompassing the *P4HB* locus have been found in apparently healthy humans,[29,30] and the ExAC database lists three premature truncating *P4HB* variants, suggesting that PDI haploinsufficiency does not cause CCS.

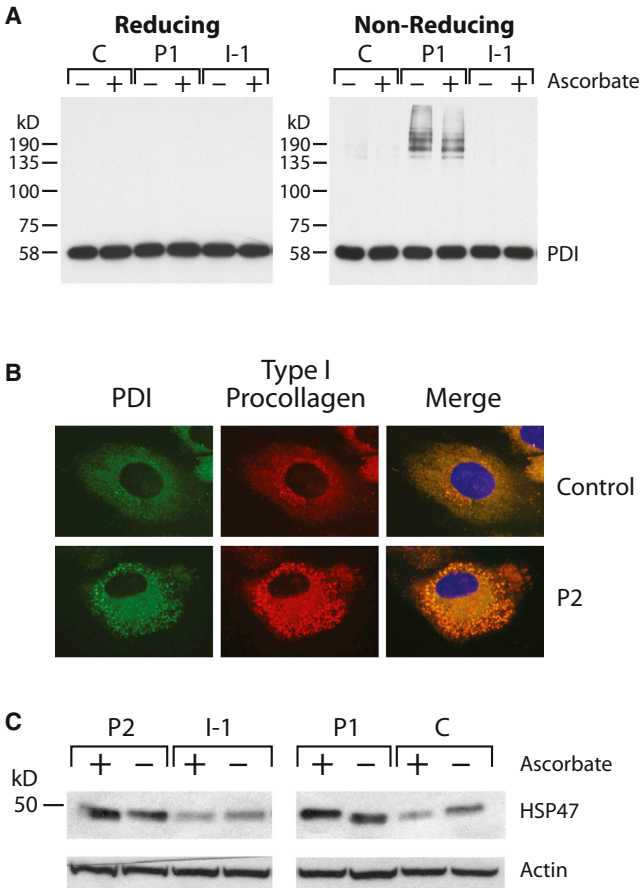

Figure 4. Protein Analyses in Skin Fibroblasts
(A) Western blot of PDI under reducing and non-reducing conditions. The amount of PDI is similar in a control (C), individual 1 (P1), and the father of individual 1 (I-1), regardless of whether ascorbate is added or not. Under non-reducing conditions (without addition of dithiothreitol, to preserve disulfide bonds), additional bands are visible in individual 1, indicating that PDI with the p.Tyr393Cys variant forms stable disulfide bridges with other proteins.
(B) Immunofluorescence. PDI and type I procollagen have a more vesicular pattern in skin fibroblasts from individual 2 (P2) as compared to the control.
(C) Western blot for HSP47. Accumulation of heat shock protein 47 (HSP47) is increased in fibroblasts from individual 1 (P1) and 2 (P2), suggesting endoplasmic reticulum stress. Ascorbate was added to the culture to stimulate collagen type I secretion. This did not have a discernible effect on HSP47 accumulation.

The fact that both individuals with CCS had the identical variant in *P4HB* and that no other *P4HB* variants have been linked to Mendelian disorders in humans also argues for the hypothesis that a gain in a specific detrimental and thus dominant-negative function is required to cause the CCS phenotype. Our immunoblot experiments of fibroblast protein extract under non-reducing conditions suggest that formation of more stable disulfide bridges with other proteins may be one of the new detrimental functions of PDI that is introduced by the p.Tyr393Cys substitution. Cys397 of PDI interacts with cysteine residues of many substrate proteins and this interaction is then released by Cys400.[31] If the Cys393 introduced by the p.Tyr393Cys variant interferes with Cys400, as modeling predicts (Figure 2D), then this release of PDI from its substrate may be delayed, potentially leading to the accumulation of substantially more PDI-substrate complexes. Such a mechanism might explain the apparently dominant-negative effect of the substitution.

Even though *P4HB* is ubiquitously expressed, the phenotype associated with the p.Tyr393Cys variant is characterized mainly by skeletal manifestations and hydrocephalus. The apparent site-specificity of the phenotype may be explained by the fact that PDI is only one member of a large family of proteins with disulfide isomerase activity.[20] It is therefore possible that PDI is particularly important for the skeleton whereas other disulfide isomerases are more prominent in other tissues.

Both individuals with CCS had a radiographic appearance of "popcorn epiphyses" in the distal femora. This presumably reflects disintegrated growth plates, a frequent finding in severe OI that might be caused by lack of structural support of growth plates by the rarefied bone tissue.[32] The fact that the individuals described here did not have an obvious clinical benefit from pamidronate therapy may be explained by the fact that they had reached skeletal maturity by the time that the treatment was started. Consequently, there was little scope for preventing bone deformities and for reshaping compressed vertebral bodies through growth.

The exact mechanistic link between the p.Tyr393Cys variant in PDI and the severe bone fragility observed in the two affected individuals remains to be elucidated. Even though PDI is thought to be important for collagen type I formation and most types of OI are characterized by collagen type I abnormalities, our evaluation of skin fibroblasts from both individuals with CCS did not reveal clear-cut disturbances in collagen type I formation. However, the phenotype of CCS suggests that the variant affects bone more than skin. It is therefore conceivable that the p.Tyr393Cys variant affects collagen processing more in osteoblasts than in skin fibroblasts.

In addition, PDI is one of the most abundant proteins in the endoplasmic reticulum.[21,31] The presence of large amounts of dysfunctional protein in the endoplasmic reticulum might have a cell-toxic effect. In accordance with this, we observed increased endoplasmic reticulum stress in skin fibroblasts and these cells also showed an altered endoplasmic reticulum pattern. Endoplasmic reticulum stress is also a prominent feature of some forms of OI that are caused by mutations in collagen type I encoding genes, in particular those that affect the C-propeptide.[33] Endoplasmic reticulum stress might lead to osteoblast apoptosis and thus defective bone formation and bone fragility, as demonstrated in an OI mouse model.[34] Conceivably, therefore, the p.Tyr393Cys variant might lead to dysfunction of bone formation through multiple pathways.

Supplemental Data

Supplemental Data include three figures and two tables and can be found with this article online at http://dx.doi.org/10.1016/j.ajhg.2014.12.027.

Acknowledgments

We thank Patty Mason for technical assistance and Mark Lepik for the preparation of the figures. F.R. received support from the Chercheur-Boursier Clinicien program of the Fonds de Recherche du Québec - Santé. J.M. is a recipient of a Canada Research Chair. We also wish to acknowledge the contribution of the high-throughput and Sanger sequencing platforms of the McGill University and Genome Québec Innovation Centre. This study was supported by the Shriners of North America.

Received: October 17, 2014
Accepted: December 29, 2014
Published: February 12, 2015

Web Resources

The URLs for data presented herein are as follows:

1000 Genomes, http://browser.1000genomes.org
dbSNP, http://www.ncbi.nlm.nih.gov/projects/SNP/
Database of Genomic Variants (DGV), http://dgv.tcag.ca/dgv/app/home
ExAC Browser, http://exac.broadinstitute.org/
Human Gene Mutation Database, http://www.hgmd.org/
GATK, http://www.broadinstitute.org/gatk/
NHLBI/NHGRI Exome Project: http://exome.gs.washington.edu/
OMIM, http://www.omim.org/
UCSC Genome Browser, http://genome.ucsc.edu

References

1. Cole, D.E., and Carpenter, T.O. (1987). Bone fragility, craniosynostosis, ocular proptosis, hydrocephalus, and distinctive facial features: a newly recognized type of osteogenesis imperfecta. J. Pediatr. *110*, 76–80.
2. Cohen, M.M., Jr. (1988). Craniosynostosis update 1987. Am. J. Med. Genet. Suppl. *4*, 99–148.
3. Amor, D.J., Savarirayan, R., Schneider, A.S., and Bankier, A. (2000). New case of Cole-Carpenter syndrome. Am. J. Med. Genet. *92*, 273–277.
4. Rauch, F., and Glorieux, F.H. (2004). Osteogenesis imperfecta. Lancet *363*, 1377–1385.
5. Warman, M.L., Cormier-Daire, V., Hall, C., Krakow, D., Lachman, R., LeMerrer, M., Mortier, G., Mundlos, S., Nishimura, G., Rimoin, D.L., et al. (2011). Nosology and classification of genetic skeletal disorders: 2010 revision. Am. J. Med. Genet. A. *155A*, 943–968.
6. Van Dijk, F.S., and Sillence, D.O. (2014). Osteogenesis imperfecta: clinical diagnosis, nomenclature and severity assessment. Am. J. Med. Genet. A. *164A*, 1470–1481.
7. Forlino, A., Cabral, W.A., Barnes, A.M., and Marini, J.C. (2011). New perspectives on osteogenesis imperfecta. Nat. Rev. Endocrinol. *7*, 540–557.
8. Marini, J.C., and Blissett, A.R. (2013). New genes in bone development: what's new in osteogenesis imperfecta. J. Clin. Endocrinol. Metab. *98*, 3095–3103.
9. Fahiminiya, S., Majewski, J., Roughley, P., Roschger, P., Klaushofer, K., and Rauch, F. (2013). Whole-exome sequencing reveals a heterozygous LRP5 mutation in a 6-year-old boy with vertebral compression fractures and low trabecular bone density. Bone *57*, 41–46.
10. Fahiminiya, S., Majewski, J., Mort, J., Moffatt, P., Glorieux, F.H., and Rauch, F. (2013). Mutations in WNT1 are a cause of osteogenesis imperfecta. J. Med. Genet. *50*, 345–348.
11. McDonald-McGinn, D.M., Fahiminiya, S., Revil, T., Nowakowska, B.A., Suhl, J., Bailey, A., Mlynarski, E., Lynch, D.R., Yan, A.C., Bilaniuk, L.T., et al. (2013). Hemizygous mutations in SNAP29 unmask autosomal recessive conditions and contribute to atypical findings in patients with 22q11.2DS. J. Med. Genet. *50*, 80–90.
12. Wang, K., Li, M., and Hakonarson, H. (2010). ANNOVAR: functional annotation of genetic variants from high-throughput sequencing data. Nucleic Acids Res. *38*, e164.
13. Christiansen, H.E., Schwarze, U., Pyott, S.M., AlSwaid, A., Al Balwi, M., Alrasheed, S., Pepin, M.G., Weis, M.A., Eyre, D.R., and Byers, P.H. (2010). Homozygosity for a missense mutation in SERPINH1, which encodes the collagen chaperone protein HSP47, results in severe recessive osteogenesis imperfecta. Am. J. Hum. Genet. *86*, 389–398.
14. Kumar, P., Henikoff, S., and Ng, P.C. (2009). Predicting the effects of coding non-synonymous variants on protein function using the SIFT algorithm. Nat. Protoc. *4*, 1073–1081.
15. Adzhubei, I.A., Schmidt, S., Peshkin, L., Ramensky, V.E., Gerasimova, A., Bork, P., Kondrashov, A.S., and Sunyaev, S.R. (2010). A method and server for predicting damaging missense mutations. Nat. Methods *7*, 248–249.
16. Schwarz, J.M., Rödelsperger, C., Schuelke, M., and Seelow, D. (2010). MutationTaster evaluates disease-causing potential of sequence alterations. Nat. Methods *7*, 575–576.
17. Ge, B., Gurd, S., Gaudin, T., Dore, C., Lepage, P., Harmsen, E., Hudson, T.J., and Pastinen, T. (2005). Survey of allelic expression using EST mining. Genome Res. *15*, 1584–1591.
18. Campbell, C.D., and Eichler, E.E. (2013). Properties and rates of germline mutations in humans. Trends Genet. *29*, 575–584.
19. Rauch, A., Wieczorek, D., Graf, E., Wieland, T., Endele, S., Schwarzmayr, T., Albrecht, B., Bartholdi, D., Beygo, J., Di Donato, N., et al. (2012). Range of genetic mutations associated with severe non-syndromic sporadic intellectual disability: an exome sequencing study. Lancet *380*, 1674–1682.
20. Benham, A.M. (2012). The protein disulfide isomerase family: key players in health and disease. Antioxid. Redox Signal. *16*, 781–789.
21. Hatahet, F., and Ruddock, L.W. (2009). Protein disulfide isomerase: a critical evaluation of its function in disulfide bond formation. Antioxid. Redox Signal. *11*, 2807–2850.
22. Pyott, S.M., Schwarze, U., Christiansen, H.E., Pepin, M.G., Leistritz, D.F., Dineen, R., Harris, C., Burton, B.K., Angle, B., Kim, K., et al. (2011). Mutations in PPIB (cyclophilin B) delay type I procollagen chain association and result in perinatal lethal to moderate osteogenesis imperfecta phenotypes. Hum. Mol. Genet. *20*, 1595–1609.
23. Myllyharju, J. (2008). Prolyl 4-hydroxylases, key enzymes in the synthesis of collagens and regulation of the response to hypoxia, and their roles as treatment targets. Ann. Med. *40*, 402–417.
24. LaMantia, M., Miura, T., Tachikawa, H., Kaplan, H.A., Lennarz, W.J., and Mizunaga, T. (1991). Glycosylation site binding protein and protein disulfide isomerase are identical and

essential for cell viability in yeast. Proc. Natl. Acad. Sci. USA *88*, 4453–4457.
25. Hahm, E., Li, J., Kim, K., Huh, S., Rogelj, S., and Cho, J. (2013). Extracellular protein disulfide isomerase regulates ligand-binding activity of alphaMbeta2 integrin and neutrophil recruitment during vascular inflammation. Blood *121*, 3789–3800, S3781–3715.
26. Kosuri, P., Alegre-Cebollada, J., Feng, J., Kaplan, A., Inglés-Prieto, A., Badilla, C.L., Stockwell, B.R., Sanchez-Ruiz, J.M., Holmgren, A., and Fernández, J.M. (2012). Protein folding drives disulfide formation. Cell *151*, 794–806.
27. Lyles, M.M., and Gilbert, H.F. (1991). Catalysis of the oxidative folding of ribonuclease A by protein disulfide isomerase: dependence of the rate on the composition of the redox buffer. Biochemistry *30*, 613–619.
28. Ishikawa, Y., and Bächinger, H.P. (2013). A molecular ensemble in the rER for procollagen maturation. Biochim. Biophys. Acta *1833*, 2479–2491.
29. Jakobsson, M., Scholz, S.W., Scheet, P., Gibbs, J.R., VanLiere, J.M., Fung, H.C., Szpiech, Z.A., Degnan, J.H., Wang, K., Guerreiro, R., et al. (2008). Genotype, haplotype and copy-number variation in worldwide human populations. Nature *451*, 998–1003.
30. Wong, K.K., deLeeuw, R.J., Dosanjh, N.S., Kimm, L.R., Cheng, Z., Horsman, D.E., MacAulay, C., Ng, R.T., Brown, C.J., Eichler, E.E., and Lam, W.L. (2007). A comprehensive analysis of common copy-number variations in the human genome. Am. J. Hum. Genet. *80*, 91–104.
31. Wilkinson, B., and Gilbert, H.F. (2004). Protein disulfide isomerase. Biochim. Biophys. Acta *1699*, 35–44.
32. Obafemi, A.A., Bulas, D.I., Troendle, J., and Marini, J.C. (2008). Popcorn calcification in osteogenesis imperfecta: incidence, progression, and molecular correlation. Am. J. Med. Genet. A. *146A*, 2725–2732.
33. Chessler, S.D., and Byers, P.H. (1993). BiP binds type I procollagen pro alpha chains with mutations in the carboxyl-terminal propeptide synthesized by cells from patients with osteogenesis imperfecta. J. Biol. Chem. *268*, 18226–18233.
34. Lisse, T.S., Thiele, F., Fuchs, H., Hans, W., Przemeck, G.K., Abe, K., Rathkolb, B., Quintanilla-Martinez, L., Hoelzlwimmer, G., Helfrich, M., et al. (2008). ER stress-mediated apoptosis in a new mouse model of osteogenesis imperfecta. PLoS Genet. *4*, e7.